

Theoretical Approach for the Design of a New Wideband Ku-band Printed Antenna

A. Harrabi^{1,2}, T. Razban¹, Y. Mahe¹, L. Osman², and A. Gharsallah²

¹ Institute of Electronic and Telecommunication of Rennes, IETR-UMR CNRS 6164
Polytechnic Engineering School of Nantes, University of Nantes, Nantes, 44603, France
amal.harrabi@univ-nantes.fr, tchanguiz.razban@univ-nantes.fr, yann.mahe@univ-nantes.fr

² Department of Physics, UR "CSEHF" 13ES37
Faculty of Sciences of Tunis, University of Tunis El Manar, 2092 Tunisia
lotfi.osman@supcom.rnu.tn, ali.gharsallah@gmail.com

Abstract — A design of a broadband Ku-band low-cost printed circuit board technology (PCB) antenna is presented in this paper. An approach was developed to enhance the bandwidth of a simple printed patch antenna. The proposed method is, step by step, detailed to discuss the evolution of the antenna geometry and depicts the contribution of the imported changes on the properties achieved each time. A 22% relative bandwidth in Ku-band was obtained for a footprint of $0.4\lambda_0 \times 0.6\lambda_0$ (λ_0 is the wavelength in the free space). A good agreement between the simulation and the measurement results of the wideband patch was observed, which proves the interest of this approach.

Index Terms — Antenna input impedance, antenna theory, Ku-band, linear polarization, polygonal antennas, wideband antenna.

I. INTRODUCTION

There is a growing interest in small, flat, discreet, efficient, and low-cost antenna design. In satellite application context, these antennas should have a broadband behavior covering all the Ku-band, a high directivity and a linear polarization. The reflector based antennas are commonly used because they satisfy all these requirements, but they are not practical due to their relatively big size and their 3D geometry. An interesting alternative of such antennas could be the grounded planar printed based antennas because of their low profile, cheap price and simple manufacturing [1,2]. Nevertheless, with such a technology for simple shape antenna, broadband behavior is limited to a few percent. To enhance the bandwidth, different techniques can be used. Some are based on the superposition of several layers of dielectrics and resonators known as the stacked antennas [3-7]. This technique implies a precise alignment of the resonators hard to achieve, especially at high

frequency like in Ku-band. Others use a co-planar arrangement of parasitic elements surrounding the driven resonator. These parasitic elements have almost the same size as the driven one which leads to a relatively large size of the patch. When high directivity has to be reached, antenna array is needed and therefore the patch size becomes a crucial criterion. In this case, if the basic element has more than a wavelength size, grating lobe problem arises. Coplanar multi-resonator solution is then irrelevant and incompatible with antenna array [8-11]. In [12] and [13], the authors explain that with some modifications of the geometry of the rectangular patch antenna, a relative bandwidth of 20% can be achieved just by coupling two different modes. The two chosen modes are orthogonal. It means that the polarization is unstable within the bandwidth. Therefore, the steady linear polarization criterion for satellite reception cannot be satisfied. In this paper, we propose to develop a new broadband single element printed antenna operating in Ku-band with compact size and stable linear polarization in order to be suitable with an antenna array configuration and achieve higher directivity. This article is organized as follows: In Section II, a rigorous theoretical approach is developed and validated according to simulations using CST Microwave Studio® software. A prototype of the proposed antenna is realized and measured. Measurement results, presented in Section III, are in good agreement compared to the simulations.

II. ANTENNA DESIGN

A. Rectangular patch antenna

Different kinds of planar antenna topologies exist: ungrounded and grounded ones. The first is interesting for its omnidirectional radiation pattern and an ultra-wideband behavior could be easily achieved. It is extensively used for applications like mobile communication systems. The second is more suitable for

point-to-point communication to avoid energy losses, except that the limited bandwidth is its handicap. As satellite services require point-to-point communication with direct link antennas, the grounded planar antenna technology is then more suitable, if solutions are found to maintain the linear polarization over a wide bandwidth. In this technology, the bandwidth usually depends on the thickness, the nature of the dielectric substrate, and the antenna's geometry. To broaden the bandwidth of a rectangular patch antenna, the most used techniques are based on decreasing the substrate relative permittivity ϵ_r , raising the dielectric thickness h and enlarging the patch width W [14]. However, the bandwidth of this simple shape printed antenna remains limited to about 10%. To highlight this issue, a probe-fed rectangular microstrip antenna printed on a 1.58 mm height Teflon-glass substrate of a relative permittivity 2.55 and $\tan\delta = 0.007$ operating at 11.7 GHz is firstly simulated with CST Microwave Studio®. Its dimensions are tuned in order to enlarge the bandwidth for this simple pattern. The optimized rectangular antenna's reflection coefficient S_{11} is represented in Fig. 1.

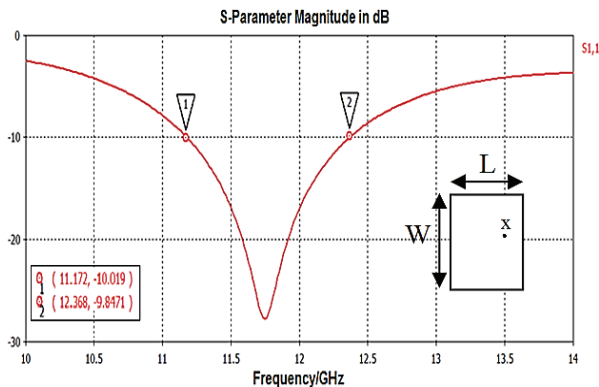


Fig. 1. Simulated reflection coefficient S_{11} of the rectangular patch antenna ($L = 7$ mm and $W = 10$ mm and $x = 2.7$ mm).

As previously mentioned, a relative bandwidth of 10% is observed in this figure, which is quite close to the maximum bandwidth for this kind of structure [14]. An idea to overcome this insufficiency consists in designing a simple patch antenna by exploring the rectangular patch characteristics and making some changes in its geometry to get an enlarged bandwidth of more than 10%, while maintaining the same linear polarization over the whole bandwidth. Therefore, a rectangular patch is introduced and analyzed. Its dimensions are calculated from the analytical expressions given in [15,16]. According to these expressions, the variation of the length L of a rectangular patch printed on a Teflon-glass substrate for fixed values of W (width of the patch), h (the substrate thickness), and ϵ_r (substrate relative permittivity) versus the frequency is represented in Fig. 2.

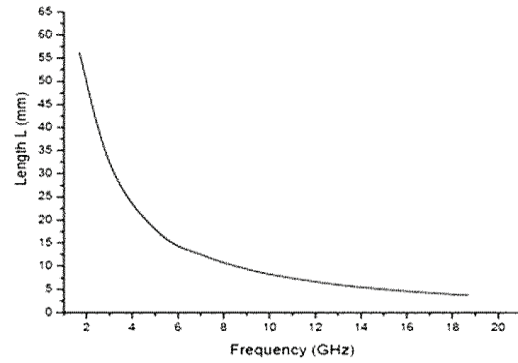


Fig. 2. Length of a rectangular patch versus frequency when $W = 13$ mm, $h = 1.58$ mm, $\epsilon_r = 2.55$ and $x = 2.7$ mm.

Internal for a rectangular patch antenna, fed by a coaxial cable at a distance x from the center of the rectangle patch, the input resistance R_i is defined in [16] by:

$$R_i = \frac{1}{2G} \sin^2\left(\frac{\pi x}{L}\right), \tag{1}$$

where

$$G = \frac{w}{120\lambda_0} \left[1 - \frac{(2\pi h/\lambda_0)^2}{24} \right], \tag{2}$$

is the radiation conductance and λ_0 is the wavelength.

According to equation (1), the value of the input resistance is related to the position x of the feed point from the center of the antenna. To get maximum power transfer, this position should be determined in a way that the input resistance R_i is equal to the source resistance (typically 50Ω). On the other hand, for a fixed distance x ; the input resistance will only depend on the frequency when W , h and ϵ_r have also fixed values as illustrated by Fig. 3 below.

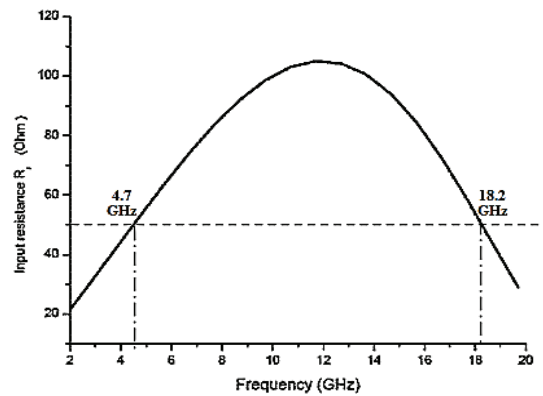


Fig. 3. Input resistance R_i (Ω) versus frequency when $W = 13$ mm, $h = 1.58$ mm, $\epsilon_r = 2.55$ and $x = 2.7$ mm.

According to Fig. 3, some same input resistance is met for two different frequencies. For example, $R_i = 50 \Omega$ is obtained at both 4.7 GHz and 18.2 GHz, which means that two collinear resonators can be optimally coupled to

the same feed point position.

B. Polygonal patch antenna

In accordance with Fig. 3, two resonators can be optimally coupled having the same feeding point; in this case, this is possible for coaxial feeding probe situated at $x = 2.7$ mm from the center of the resonators. Based on Fig. 2, the first resonator has 3.9 mm length for a frequency of 18.2 GHz and the second has 19.2 mm length for a frequency of 4.7 GHz. We should then present a geometry that has these two different lengths. One way consists in using the dimensions L and W of the patch antenna as L_1 and L_2 . But, in this case, two orthogonal modes are excited, which means that the radiated power has different polarizations. To ensure same polarizations over the two frequencies, L_1 and L_2 has to be carried on along only one axis. As illustrated in Fig. 4 (a), a polygonal design can be a possible candidate to meet the mentioned condition of the linear polarization using the two different lengths. From Fig. 3, the expected reflection coefficient S_{11} of this antenna should have the form given in Fig. 4 (b).

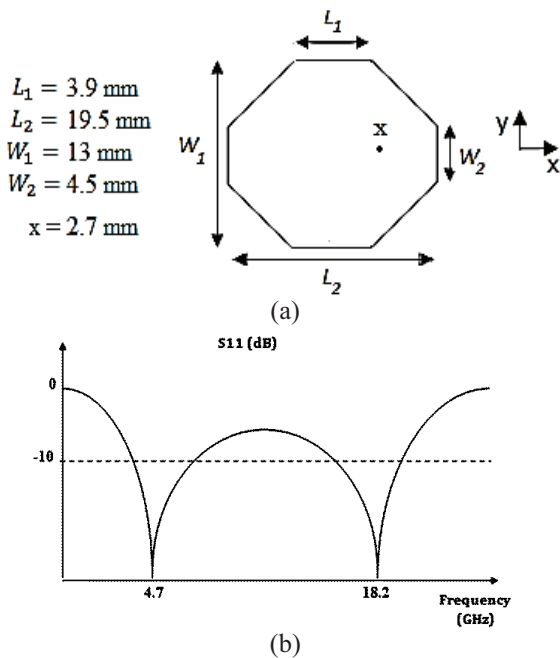


Fig. 4. Proposed antenna and its expected reflection coefficient: (a) polygonal patch antenna, and (b) S_{11} parameter of the polygonal antenna matched to 50Ω .

In order to reduce the size of the polygonal antenna, to widen the bandwidth of each resonant frequency and to have protection against the environment, a 3.175 mm thickness Nelco NY9220 substrate with a relative permittivity of 2.2 and $\tan \delta = 0.0009$ is used as a rodome. To take into account the rodome layer effect in the simulation, we need an optimization of the polygonal

antenna dimensions. Figure 5 shows the dimensions of the antenna with superstrate and the simulation result of its S_{11} parameter.

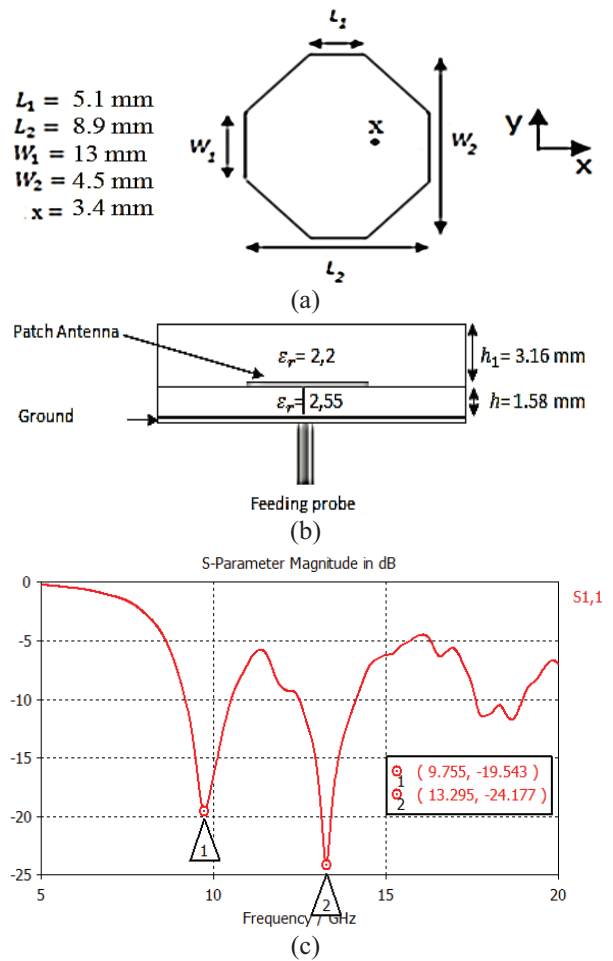
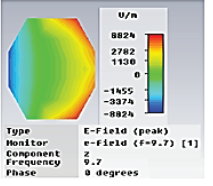
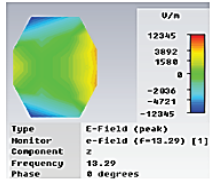
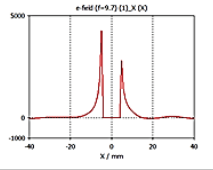
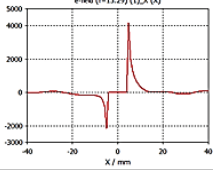
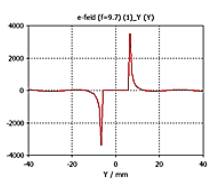
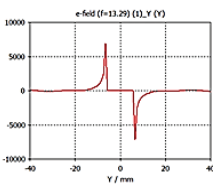


Fig. 5. (a) Dimensions of the polygonal antenna with rodome, (b) side view, and (c) simulated S_{11} parameter.

This figure confirms that the optimized antenna with rodome has a dual band behavior. Table 1 summarizes the electric field distribution for the two resonant frequencies to check their polarizations quality.

We notice that for all these two dips, the transverse fringing fields along Y-axis (E_y) on both sides of the antenna are in opposite phase with quite the same magnitude. In other words, the resulted vertical polarization radiation (cross-polarization) in the broadside direction is null for all frequencies, meaning that the polygonal shape of the patch does not introduce theoretically any cross-polarization. For the frequencies 9.75 and 13.29 GHz, the electric fields along X-axis are not in opposite phase, so the resulted radiation horizontal polarization (co-polarization) is maximal in the broadside direction.

Table 1: E-field of the polygonal antenna with rodome

Frequency (GHz)	9.75	13.29	
	I	II	
E_z			a
E_x			b
E_y			c

C. Polygonal antenna with circular slot

The polygonal antenna depicted in Fig. 5 presents two separated bands corresponding to two distinct modal resonances. Nevertheless, wideband behavior is expected. From Fig. 3, the impedance plot presents a maximum for a frequency located between the two frequencies matched to 50 Ω, which explains the high reflection coefficient for this distinct frequency. The idea consists of reducing the reflection coefficient at this maximum without deteriorating the impedance matching of the existing two frequencies. It can be resolved by modifying the propagation conditions inside the resonator. Thus, follows a manner to enlarge the bandwidth by using a slot inside the polygonal patch is step by step detailed.

1) Influence of a slot inside the patch

First, it is important to review theoretically the effect of a simple slot inside a patch. Usually, a slot can be modeled as a capacitance whose value depends not only on the dimension of the slot, but also on its orientation and its position inside the patch. To evaluate the influence of the slot, the electric field distribution inside the substrate, under the patch, is studied. For the fundamental resonance of a rectangular patch antenna, the magnitude of the electric field is expressed in [16] as follows:

$$E = E_0 \sin \frac{\pi x}{L}, \tag{3}$$

where E_0 is the maximum electric field and x is between $\frac{-L}{2}$ and $\frac{L}{2}$.

The fringing field at the edge of the patch is the origin of its radiation. Its magnitude E_r can be determined

by the equivalent potential:

$$E_r = \frac{E_0 h}{\Delta}, \tag{4}$$

where h is the thickness of the substrate and Δ the line extension the resonators from both sides.

With a slot inside the antenna at a distance d from the center of the patch, an electric field \vec{E}_s appears inside the slot, Fig. 6.

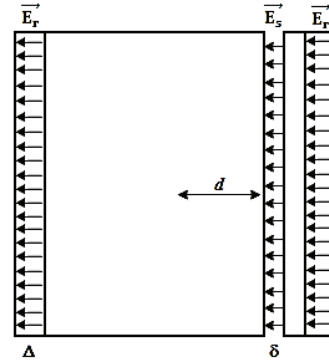


Fig. 6. Electric fields E_r and E_s .

The value of the magnitude of this electric field can be determined by calculating the potential difference between both sides of the slot:

$$E_s \delta = V_2 - V_1, \tag{5}$$

where δ is the slot width, V_1 is the potential at $y = d$ and V_2 is the potential at $y = d + \delta$.

Assuming that $d \gg \delta$ and $\delta \ll L$, then:

$$E_s = E_0 \frac{\pi h}{L} \cos \frac{\pi d}{L}. \tag{6}$$

From the expression of the electric field magnitude E_s , we deduce that E_s is much smaller than E_r because L is much bigger than Δ . Therefore, the slot does not have great influence on the radiation pattern of the antenna. Now, if the slot is oriented with an angle θ , Fig. 7, E_s can be written as follows:

$$E_s(y) = E_0 \left[\frac{\pi h \cos \theta}{L} \cos \frac{\pi d}{L} \right], \tag{7}$$

where d is the distance between the Y-axis of the patch and the slot location for a given value of y .

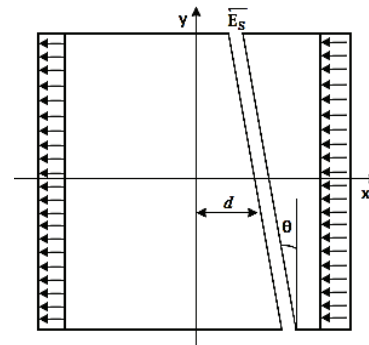


Fig. 7. Representation of the slot with an angle θ .

To maintain the symmetry of the structure, we propose to use a circular slot. In this case, the distance d will depend on the angle θ and the inner radius R of the circular slot and can be written as follows:

$$d = R \cos \theta, \quad (8)$$

where θ varies from 0° to 360° , Fig. 8.

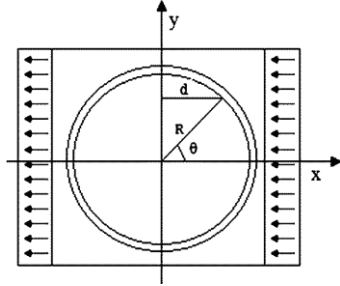


Fig. 8. Variation of the distance d in a circular slot.

Finally, the magnitude of the electric field inside the slot has the following expression:

$$E_s = E_0 \frac{\pi h}{L} \cos\left(\frac{\pi R \cos \theta}{L}\right) \cos \theta, \quad (9)$$

Fig. 9 represents the variation of E_s versus θ according to the equation (9).

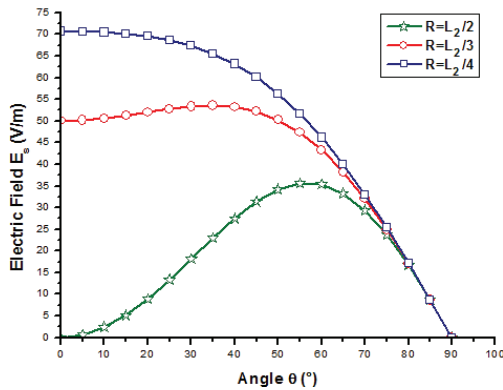


Fig. 9. Variation of the magnitude of the electric field inside the circular slot E_s versus theta (θ) for different values of the slot radius R when $E_0 \frac{\pi h}{L} = 100$.

To explain the circular slot influence, we consider the patch antenna as a transmission line [16]. From this model, the input impedance is related to the characteristic impedance of the line which is given by the following expression:

$$Z_c = \sqrt{\frac{L_0}{C_0}}, \quad (10)$$

where L_0 is the serial inductance per unit length and C_0 is the parallel capacitance per unit length.

When a slot is introduced inside the patch antenna, its equivalent capacitance C_s reduces the serial inductance L_0 and so the characteristic impedance of the line,

assuming that the phase velocity of the travelling wave remains unchanged. From Fig. 9, we notice that the value of the electric field E_s inside the circular slot is non-null, when theta (θ) is within the range $[0^\circ, 90^\circ]$ and it is null when $\theta = 0^\circ$ or $\theta = 90^\circ$ for $R \approx \frac{L}{2}$. In this case, the capacitance C_s is equal to zero when theta's value is equal to 0° or 90° , due to the absence of the electric field for these two values of theta. Therefore, the slotted patch characteristic impedance Z'_c at $\theta = 0^\circ$ and $\theta = 90^\circ$ is almost equal to the patch characteristic impedance Z_c without slot. But, its value decreases when θ is within the range of degrees from 0° to 90° .

In section I, we demonstrated that for a polygonal antenna, the lower resonant frequency is related to the largest length (L_2) and the higher one is related to the smallest length (L_1). Now, after the insertion of the circular slot, when $\theta = 0^\circ$, a portion of the slot is located on the largest length. But when $\theta = 90^\circ$, another portion is located on the smallest length. It is then expected, theoretically and based on the discussion following Fig. 9 that the circular slot will not impact the impedance matching for the two resonant frequencies of the antenna presented in Fig. 5. However, the frequencies between them undergo an input resistance reduction, which should improve the bandwidth of the antenna.

2) Simulation results

A polygonal antenna with a circular slot inside the patch [17] has been simulated and it is shown in Fig. 10. According to the previous theory, the value of the outer radius R_{out} is chosen close to $\frac{L_2}{2}$ ($R_{out} = 3.7$ mm). The slot width is equal to 0.3 mm. The feeding probe is located at a distance $x = 2.9$ mm from the center of the antenna. A small air gap of 0.1 mm needs to be taken into account in the simulation between the patch and the rodome. The simulation result of S_{11} parameter of the proposed antenna is given in Fig. 11.

According to the simulation result for the given value of the slot width (0.3 mm), this antenna has a bandwidth around 3 GHz (from 11.6 GHz to 14.8 GHz) at -10 dB. The simulation shows that due to the insertion of the circular slot, the dual band antenna was indeed transformed to a broadband antenna.

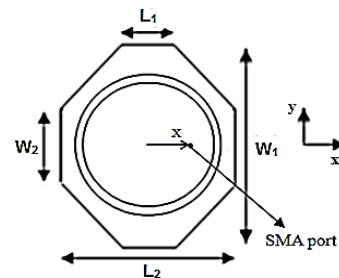


Fig. 10. Proposed polygonal antenna with a circular slot.

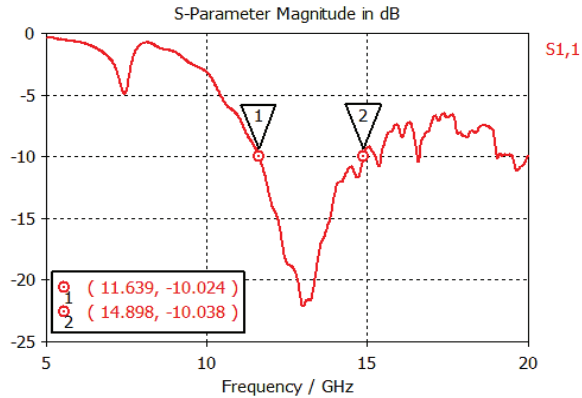


Fig. 11. Simulation result of the S_{11} parameter of the antenna patch with circular slot.

To show the influence of the slot width on the antenna reflection coefficient, a parametric study for different widths of the circular slot (quite small compared to the wavelength) is given in Fig. 12.

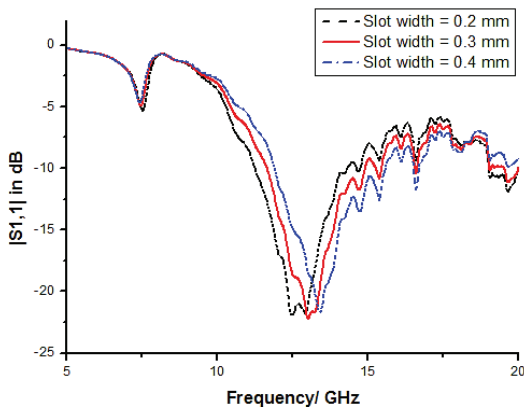


Fig. 12. Parametric study for different widths of the circular slot.

Table 2 shows that the relative bandwidth of the proposed antenna is not highly affected by the slot width which remains around 20%. Only the central frequency shifts towards higher frequencies as the slot width increases.

Table 2: Antenna relative bandwidth for different slot width

Slot Width (mm)	Relative Bandwidth (%)	Central Frequency (GHz)
0.2	21	12.75
0.3	21	13.2
0.4	22	13.7

This is mainly due to the changes in the phase velocity supposed to be constant in the theory. The E-fields of the circular slotted polygon at 11.63 GHz, 13 GHz, and at 14.8 GHz are provided in Table 3 below.

The electric field distribution symmetry observed for all frequencies within the bandwidth, shows that the resulted field is oriented along X-axis and that the cross-polarization theoretically is null due to its perfect symmetry.

Table 3: E-field of the polygonal antenna with circular slot

Frequency (GHz)	11.63	13	14.8	
	I	II	III	
E_z				a
E_x				b
E_y				c

According to Table 3 comments, the simulated co/cross-polarization radiation pattern, given in Table 4, shows that the cross-polarization level is about 20 dB less than the main polarization, as expected. The same polarization is observed over the whole bandwidth.

Table 4: Co/Cross-polarization in the E-plane at different frequencies

Frequency (GHz)	Co/Cross-polarization		Co/Cross-polarization
	11.6	13	

III. PROTOTYPE AND MEASUREMENTS

A prototype of this antenna was manufactured and measured. The dimensions of this design are given in Table 5. The patch was printed on a Teflon-glass substrate of 1.58 mm thickness with a relative permittivity of 2.55 and $\tan\delta = 0.007$. Its dimensions are set to $50 \times 50 \text{ mm}^2$ ($2\lambda_0 \times 2\lambda_0$, where λ_0 is the wavelength at the lower frequency

10.7 GHz).

Table 5: Prototype antenna dimensions

Parameter	Value (mm)
L_1	5.1
W_1	13
L_2	8.9
W_2	4.5
R_{in} (the slot inner radius)	3.41
R_{out} (the slot outer radius)	3.72
Feeding probe at x	2.9

The used rodome is a Nelco NY9220 substrate of a 3.175 mm thickness with a relative permittivity of 2.2 and $\tan\delta = 0.0009$. The total size of the antenna is near $0.4\lambda_0 \times 0.6\lambda_0$, compatible for the design of an antenna array. A photo of the proposed antenna is given in Fig. 13.



Fig. 13. Photo of the prototype antenna.

As shown in Fig. 14, a good agreement between simulations and measurements in terms of bandwidth is observed. It is around 3 GHz at -10 dB, which represents a relative bandwidth of 22%. The difference between the simulated and measured S_{11} is mainly due to the manual fabrication of the prototype, especially the feeding probe drilling (about few hundred μm).

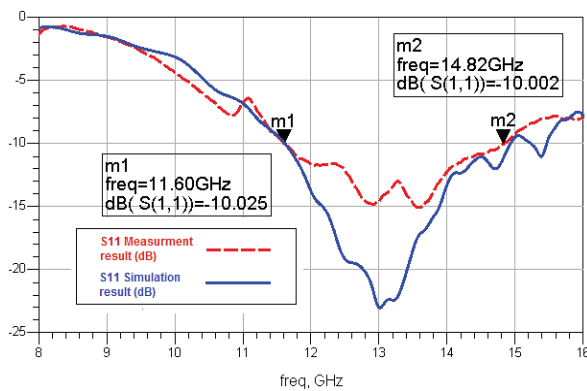


Fig. 14. Comparison of S_{11} parameter of the simulated and measured antenna.

Figure 15 below presents the measured radiation pattern of the antenna. The main and the cross-polarizations in E- and H-planes are given for three frequencies inside the band.

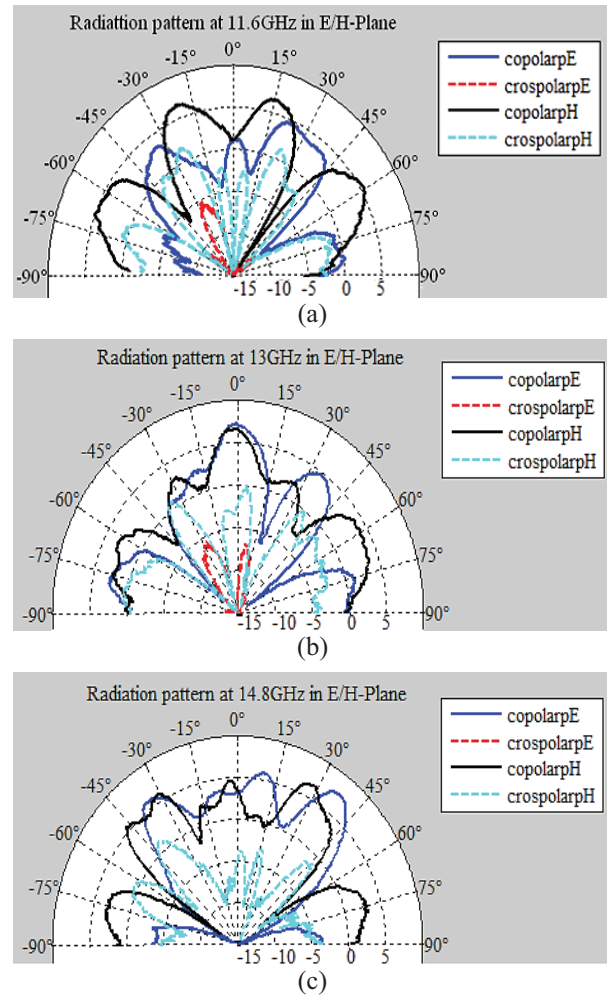


Fig. 15. Radiation pattern measurements within the bandwidth.

In the main radiation direction, the cross-polarization is about 10 dB lower than the main polarization. However, a slight degradation of the co/cross-polarization level is observed as we move away from broadside direction, particularly observed at lower frequencies of the bandwidth.

The reason behind this result could arise from the prototyping technology and maybe the zero-scale balance of the feeding probe problem due to the manual drilling. The observed ripples in the radiation pattern for all frequencies can be explained by the diffraction of the radiated field on the ground plane because of its limited dimensions. The maximum directivity observed is about 6.4 dBi.

IV. CONCLUSION

In this paper, a theoretical approach of an original broadband antenna design is presented. It consists of a polygonal antenna with a circular slot inside. A polygonal antenna presents initially a dual band behavior due to two different collinear resonant lengths. But, the insertion of a circular slot transforms it to a broadband behavior because this slot acts as an impedance regulator. The measurements agree well with the simulations and confirm the interesting properties of this design such as the wideband behavior (a relative bandwidth of 22% in the Ku-band is observed) and the guaranteed linear polarization over the entire bandwidth. With only a footprint of $0.4\lambda_0 \times 0.6\lambda_0$ and a 6.4 dBi gain, this design is a good candidate for antenna array configuration to achieve high gain like in satellite application services.

REFERENCES

- [1] V. Peshlov, R. Traykov, G. Bozmarova, M. Popova, D. Vasilev, and Z. Ivanov, "Low-cost scanning antenna for satellite reception," *IEEE International Symposium on Phased Array Systems and Technology*, Massachusetts, USA, pp. 441-445, 2003.
- [2] U. H. Park, K. H. Lee, and S. I. Jeon, "A novel mobile antenna for Ku-band satellite communications," *ETRI Journal*, vol. 27, no. 3, June 2005.
- [3] A. Sabban, "A new broadband stacked two-layer microstrip antenna," *Proc. IEEE Antennas Propagation Sympo. Dig.*, pp. 63-66, 1983.
- [4] W. Elhaji, F. Gallee, and C. Person, "Bi-access tri-band wideband antenna for an opportunistic communication between 4G terminals," *IEEE International Symposium on Antennas and Propagation*, Spokane, United States, 2011.
- [5] A. B. Nandgaonkar and S. B. Deosarkar, "Design of high gain two-layer electromagnetically coupled patch antenna in the ISM band," *International Conference on Electromagnetics in Advanced Applications*, Torino, Italy, pp. 547-550, 2007.
- [6] J. Granholm and K. Woelders, "Dual polarization stacked microstrip patch antenna array with very low cross-polarization," *IEEE Transactions on Antennas and Propagation*, vol. 49, no. 10, Oct. 2001.
- [7] R. Wansch, H. Adel, and H. Humpfer, "Mini-terminal - a small antenna for satellite reception," *INICA*, pp. 153-157, 2007.
- [8] F. F. Dubrovka and S. Y. Martynyuk, "Wideband dual polarized planar antenna arrays," *Int. Conference on Antenna Theory and Techniques, Dept. of Theoretical Fundamentals Radio Engineering, Kiev Polytechnic Institute*, National Technical University of Ukraine, Sevastopol, Ukraine, pp. 91-96, Sep. 9-12, 2003.
- [9] S. Bouaziz, A. Ali, S. Hebib, and H. Aubert, "Planar wideband microstrip antenna with inclined radiation pattern for C-band airborne applications," *The 4th European Conference on Antennas and Propagation (EuCAP)*, Barcelone-Spain, pp. 1-4, 2010.
- [10] K. Ito, K. Ohmaru, and Y. Konishi, "Planar antenna for satellite reception," *IEEE Transactions on Broadcasting*, vol. 34, no. 4, Dec. 1988.
- [11] Z. Haiyang, M. Yann, and R. Tchanguiz, "A novel wideband and dual-polarized cross-antenna for satellite communications," *Proceedings of the Progress in Electromagnetics Research Symposium*, Stockholm, Sweden, pp. 1425-1428, Aug. 2013.
- [12] M. Manzani, A. Alu, F. Bilotti, and L. Vegni, "Design of polygonal antennas with a broad-band behavior via a proper perturbation of conventional rectangular radiators," *IEEE Antennas and Propagation Society International Symposium*, vol. 2, pp. 268-271, 2003.
- [13] M. Manzini, A. Alu, F. Bilotti, and L. Vegni, "Polygonal patch antenna for wireless communications," *IEEE Transactions on Vehicular Technology*, vol. 53, no. 5, Sep. 2004.
- [14] C. A. Balanis, *Microstrip Antennas: in Antenna Theory Analysis and Design*, John Wiley & Sons, New York, Second Edition, 1997.
- [15] Z. N. Chen and M. Y. W. Chia, *Broadband Microstrip Patch Antenna: in Broadband Planar Antennas Design and Applications*, John Wiley & Sons, 2006.
- [16] CST Microwave Studio, Version 2008, Computer Simulation Technology, Framingham, MA, 2008.



Amal Harrabi was born in November 1986. She received the Ph.D. degree in Electrical Engineering jointly from the University of Nantes, France and the University of Tunis-El Manar, Tunisia in June 2015. Her research interests include antenna design, antenna miniaturization, antenna array design and RF circuits design.



Tchanguiz Razban was born in Tabriz, Iran, in 1956. He received the Engineering degree from University of Tehran, Iran, in 1980. He received the Ph.D. and Doctorat d'Etat from the Institut National Polytechnique de Grenoble (INPG), France, in 1983 and 1989, respectively. He is currently a Full Professor of Electrical Engineering at

Ecole Polytechnique de Nantes. Since 1999 he has been the Chief Manager of the Electrical Engineering Department, Deputy Director and finally Director of Ecole Polytechnique until January 2010. His research interests include MMIC's and printed circuits for wireless communications, smart antennas and optical-microwave interfaces



Yann Mahé was born on June 29, 1973. He received the Ph.D. degree in Electrical Engineering from the University of Nantes, Nantes, France, in 2001. He is now an Assistant Professor at the Polytechnic School of the University of Nantes, Nantes, France. He is also a Researcher with

Institut d'Electronique et Telecommunications de Rennes (IETR) of Nantes, France. His research interests include antenna design, development of miniaturized and tuneable antenna for MIMO systems, multi-function antennas and antenna array design



Lotfi Osman was born in 1958 in Mahdia, Tunisia. He received his Master's degree in Automation from Lille 1 University, Science and Technology, France in 1984 and his Ph.D. in Automation and Computer Engineering in 1987 at the same University. In June 2013, he obtained

the Habilitation Degree in Electronics and Microelectronics from INSAT, National Institute of Applied Sciences and Technology in Tunis, University of Carthage, Tunisia. He is currently Assistant Professor with the Department of Electronics, Physics and Propagation at Sup'Com, Higher School of Communication of Tunis. In 2004, he joined the Unit of Research in High Frequency Electronic Circuits and Systems at the Faculty of Sciences of Tunis, University of Tunis El Manar. His current research interests include antennas and modeling in microwave integrated circuits. He is also involved with experimental characterization and antenna measurement.



Ali Gharsallah was born in 1959 in Kerkenah, Tunisia. He is Professor at the Faculty of Sciences of Tunis and Head of Research Unit "CSEHF" (code 13ES37) at the Department of Physics of the Faculty of Sciences of Tunis - University of Tunis El Manar.

He now occupies the post of Director General of Technological Studies at the Ministry of Higher Education and Scientific Research. He received the Engineering's degree in Radio Electrical from the Higher School of Telecommunications of Tunis in 1986 and the Ph.D. degree in 1994 from the National Engineering School of Tunis. Since 1991, he was with the Department of Physics at the Faculty of Sciences of Tunis. His current research interests include antennas, multi-layered structures and microwave integrated circuits.